System Reliability Analysis with Autocorrelated Kriging Predictions

Hao Wu[1,2]

Graduate Research Assistant

1. Department of Mechanical and Energy Engineering

Indiana University - Purdue University Indianapolis,

799 W. Michigan Street

Indianapolis, IN 46202

2. School of Mechanical Engineering

Purdue University

West Lafayette, IN, 47907, United States

E-mail: wu1508@purdue.edu

Zhifu Zhu

Missouri University of Science and Technology

400 West 13th Street

Rolla, MO 65401

E-mail: zzgc5@mst.edu

Xiaoping Du

Professor

Department of Mechanical and Energy Engineering

Indiana University - Purdue University Indianapolis,

799 W. Michigan Street

Indianapolis, IN 46202

E-mail: duxi@iu.edu

Abstract

When limit-state functions are highly nonlinear, traditional reliability methods, such as the first order and second order reliability method, are not accurate. Monte Carlo simulation (MCS), on the other hand, is accurate if a sufficient sample size is used, but is computationally intensive. This research proposes a new system reliability method that combines MCS and the Kriging method with improved accuracy and efficiency. Accurate surrogate models are created for limit-state functions with the minimal variance in the estimate of the system reliability, thereby producing high accuracy for the system reliability prediction. Instead of employing global optimization, this method uses MCS samples from which training points for the surrogate models are selected. By considering the autocorrelation of a surrogate model, this method captures the more accurate contribution of each MCS sample to the uncertainty in the estimate of the serial system reliability and therefore chooses training points efficiently. Good accuracy and efficiency are demonstrated by four examples.

1. INTRODUCTION

With the increasing complexity of engineering systems, the cost of system failures may also increase. In order to maintain low lifecycle cost and avoid tragic system failures, it is vital to predict the system reliability accurately in the design process. System reliability is the probability that a system performs its intended function without failures under given working conditions. With the system reliability available, designers can make more reliable decisions on maintenance plans, warranty policies, and cost assessment [1, 2].

In general, system reliability methods are classified into two major groups: analytical methods and sampling-based methods. The most popular analytical methods are the First and Second Order Reliability Methods (FORM and SORM) [3-6], which employ a first and second order approximation, respectively, to a limit-state function in the vicinity of the Most Probable Point (MPP). But for limit-state functions that are not linear or quadratic, significant errors could be introduced by FORM and SORM. Both methods may also produce larges errors if multiple MPPs exist.

Higher accuracy can be achieved by sampling-based methods. They include Monte Carlo simulation [7] and importance sampling [8-13]. MCS is widely used due to its easy implementation and high accuracy if a sufficiently large number of samples is used. MCS can deal with problems with almost any level of nonlinearity, but the computational cost is extremely high if reliability is high. Importance sampling methods could be used to reduce the computational cost because they generate more samples in the failure region. Most importance sampling methods require the MPP to center the sample distributions at the MPP. For a large-scale problem, searching for the MPP is expensive, and this reduces the efficiency of importance sampling.

In addition to the above two groups of methods, surrogate-based methods are increasingly used due to their ability of reducing computational cost by creating surrogate models, or meta-models [14, 15]. A surrogate model is a computationally inexpensive model created to substitute the original expensive limit-state function. The goal of metamodeling is to make the surrogate model accurate at an affordable computational cost. The general process of metamodeling starts with generating a small number of initial sample points (training points or TPs) by Design of Experiments (DOE) [16]. Based on these samples, an initial surrogate model is built by a metamodeling technique. Then more TPs are added to improve the accuracy of the surrogate model. Learning functions are employed to select the best TPs intelligently and the surrogate model is refined in a most efficient manner.

Popular metamodeling techniques include the polynomial response surface method [17, 18], neural networks [19-21], support vector machines [22-24], polynomial chaos expansion [25], Kriging [26-28], etc. Kriging method could be used for interpolation. The prediction of an existing training point produces the exact value of the response at the point. Besides, due to its stochastic characteristics, Kriging provides not only the prediction of an untried point, but also the variance of the prediction. The variance indicates the uncertainty of the prediction. Based on Kriging, Jones et al. developed the Efficient Global Optimization (EGO) method [29]. EGO uses the Expected Improvement Function (EIF) to achieve a good balance between exploiting areas of the design space where good solutions have been found, and exploring the design space where the uncertainty is high. Later, Bichon et al. proposed the Efficient Global Reliability Analysis (EGRA) [30] and extended it to system reliability prediction with multiple failure modes [31]. The latter method is call EGRA-SYS. The method uses the Expected Feasibility Function (EFF) to choose new TPs in the vicinity of the limit state and helps build an accurate surrogate model with less function

evaluations. EGRA needs global optimization to find the optimum training point. Recently, Echard et al. proposed an active learning method to avoid global optimization. The method takes advantage of Kriging and Monte Carlo simulation (AK-MCS) [32], which chooses new TPs from a pre-sampled MCS population. As a result, no global optimization is needed. Fauriat and Gayton then applied AK-MCS to system reliability analysis [33].

The above methods make the Kriging predictions without exploiting the covariance between pairs of given points. We referred to them as Independent Kriging Methods (IKM). As a matter of fact, the predictions from Kriging are realizations of a Gaussian process and therefore are dependent on one another. Considering the dependence could further improve the efficiency and accuracy of the active learning methods, Zhu and Du proposed a reliability method with MCS and dependent Kriging predictions, called Dependent Kriging Method (DKM) [34]. Accounting for dependence between Kriging predictions and focusing directly on the accuracy of reliability estimation, DKM achieves better accuracy and efficiency.

DKM is applicable only for component reliability analysis. The objective of the present study is to extend DKM to system reliability analysis. The contributions of this study include the following: (1) the extension of the component DKM to system problems so that multiple failure modes can be considered, (2) a new learning function that uses selected candidate points to relieve the computational burden greatly without jeopardizing the accuracy of reliability estimation, and (3) the development of a numerical procedure allows for accurate system reliability prediction at an affordable cost.

Since the proposed method is based on Kriging and DKM, we briefly review them in Section 2. In Section 3, the dependent Kriging method for systems (DKM-SYS) is explained in detail.

Section 4 provides four examples to illustrate the implementation process and the effectiveness of the new method. Conclusions are made in Section 5.

2 LITERATURE REVIEW

In this work, the component reliability is defined by

$$R = \Pr\{y = g(\mathbf{x}) > 0\} \tag{1}$$

where y is a component response and $\mathbf{x}$ is a random vector. If $y > 0$, the failure mode does not occur; otherwise, the failure occurs.

Next we herein review the methods that are needed by the proposed method.

2.1 Kriging method

Kriging is an interpolation method since its prediction at an existing TP is the exact value of the response at the point. For a performance function $y = f(\mathbf{x})$, Kriging considers $y = f(\mathbf{x})$ being a realization of Gaussian process defined by

$$G(\mathbf{x}) = \mathbf{f(x)}^{\mathrm{T}}\boldsymbol{\beta} + Z(\mathbf{x}) \tag{2}$$

where $\mathbf{f(x)}^{\mathrm{T}}\boldsymbol{\beta}$ is a determination term for the mean response, $\mathbf{f}(\mathbf{x})$ is a vector of regression functions, and $\boldsymbol{\beta}$ is a vector regression coefficient. $Z(\cdot)$ is a stationary Gaussian process with zero mean and covariance

$$Cov[Z(\mathbf{x}_i), Z(\mathbf{x}_j)] = \sigma_Z^2 R(\mathbf{x}_i, \mathbf{x}_j) \tag{3}$$

where σ_Z^2 is the process variance, and $R(\cdot,\cdot)$ is the correlation function. The commonly used Gaussian correlation is the anisotropic squared exponential model, which is given by

$$R(\mathbf{x}_i, \mathbf{x}_j) = \exp\left[-\sum_{k=1}^{d} \theta_k (x_{ik} - x_{jk})^2\right] \tag{4}$$

where x_{ik} and x_{jk} are the *k*-th components of $\mathbf{x}_i$ and $\mathbf{x}_j$, respectively, *d* is the dimensionality of $\mathbf{x}$, and θ_k is a parameter that indicates the correlation between the points in dimension *k*. Due to the stochastic characteristics, Kriging provides not only the prediction at an untried point but also the variance of the prediction. The variance indicates the uncertainty of the prediction. At an untried point **x**, the Kriging predictor $\hat{g}(\mathbf{x})$ follows a Gaussian distribution denoted by

$$\hat{g}(\mathbf{x}) \sim N(\mu_G(\mathbf{x}), \sigma_G^2(\mathbf{x})) \tag{5}$$

where $\mu_G(\mathbf{x})$ and $\sigma_G^2(\mathbf{x})$ are the prediction and its variance, respectively. They are computed by [26]

$$\mu_G(\mathbf{x}) = \mathbf{f}(\mathbf{x})^{\mathrm{T}}\hat{\boldsymbol{\beta}} + \mathbf{r}(\mathbf{x})\mathbf{R}^{-1}(\mathbf{y} - \mathbf{F}\hat{\boldsymbol{\beta}}) \tag{6}$$

$$\sigma_G^2 = \hat{\sigma}_Z^2\{1 - \mathbf{r}(\mathbf{x})^{\mathrm{T}}\mathbf{R}^{-1}\mathbf{r}(\mathbf{x}) + [\mathbf{F}^{\mathrm{T}}\mathbf{R}^{-1}\mathbf{r}(\mathbf{x}) - \mathbf{f}(\mathbf{x})]^{\mathrm{T}}(\mathbf{F}^{T}\mathbf{R}^{-1}\mathbf{F})^{-1}[\mathbf{F}^{\mathrm{T}}\mathbf{R}^{-1}\mathbf{r}(\mathbf{x}) - \mathbf{f}(\mathbf{x})]\} \tag{7}$$

in which $\mathbf{y}$ is a vector of responses at the TPs, $\mathbf{F}$ is a $m \times p$ matrix with rows $\mathbf{f}(\mathbf{x})^{\mathrm{T}}$, *m* is the number of TPs, and $\mathbf{r}(\cdot)$ is the correlation vector containing the correlation between $\mathbf{x}$ and each of the TPs.

$$r(x) = [R(\mathbf{x}, \mathbf{x}_1), R(\mathbf{x}, \mathbf{x}_2), ..., R(\mathbf{x}, \mathbf{x}_m)]^{\mathrm{T}} \tag{8}$$

$\mathbf{R}$ is the correlation matrix, which is composed of correlation functions evaluated at each possible combination of the *m* TPs. $\mathbf{R}$ is given by

$$\mathbf{R} = [R(\mathbf{x}_i, \mathbf{x}_j)],\ 1 \le i \le m; 1 \le j \le m \tag{9}$$

$\hat{\boldsymbol{\beta}}$ is the least square estimate of $\boldsymbol{\beta}$ given by

$$\hat{\boldsymbol{\beta}} = (\mathbf{F}^{\mathrm{T}}\mathbf{R}^{-1}\mathbf{F})^{-1}\mathbf{F}^{\mathrm{T}}\mathbf{R}^{-1}\mathbf{y} \tag{10}$$

and $\hat{\sigma}_Z^2$ are determined through

$$\hat{\sigma}_Z^2 = \frac{1}{m}(\mathbf{y} - \mathbf{F}\hat{\boldsymbol{\beta}})^{\mathrm{T}} \mathbf{R}^{-1}(\mathbf{y} - \mathbf{F}\hat{\boldsymbol{\beta}}) \tag{11}$$

The parameters θ_k are determined through the maximum likelihood estimation, details of which are available in Ref. [26, 27].

2.2 Review of AK-SYS and EGRA-SYS

Both AK-SYS [33] and EGRA-SYS [31] are system reliability methods and are based on the Kriging method. Once surrogate models of all the limit-state functions are built, the two methods use MCS to estimate the system reliability using the surrogate models. They at first generate a sufficient number of sample points $\mathbf{x}_{MCS}$ by MCS and use a few initial TPs to create initial surrogate models. New TPs are then added one by one so that the surrogate models are continually updated. AK-SYS and EGRA-SYS select new TPs using the strategies in AK-MCS [32] and EGRA [30], respectively. AK-MCS selects a new TP with a learning function defined by

$$U(\mathbf{x}) = \frac{\left|\mu_g(\mathbf{x})\right|}{\sigma_g(\mathbf{x})} \tag{12}$$

U is related to the chance of making a mistake on the sign of the prediction. The smaller is U, the higher is the likelihood. Consequently, the sample point with the smallest U is selected as a new TP. For a system with multiple components, a composite learning function U^* is used by AK-SYS [33] and is given by $U^*(\mathbf{x}) = \left|\mu_g^*(\mathbf{x})\right| \big/ \sigma_g^*(\mathbf{x})$. For a series system, $\mu_g^*(\mathbf{x})$ is the minimal value among the predictions of all components at $\mathbf{x}$, and $\sigma_g^*(\mathbf{x})$ is the corresponding standard deviation. EGRA-SYS [31] uses a different learning function, which is called the expected feasibility function (*EFF*) and is defined by

$$
\begin{aligned}
EFF(\mathbf{x}) = (\mu_g^*(\mathbf{x}) - e)\left[2\Phi\left(\frac{e-\mu_g^*(\mathbf{x})}{\sigma_g^*(\mathbf{x})}\right) - \Phi\left(\frac{e^- - \mu_g^*(\mathbf{x})}{\sigma_g^*(\mathbf{x})}\right) - \Phi\left(\frac{e^+ - \mu_g^*(\mathbf{x})}{\sigma_g^*(\mathbf{x})}\right)\right] \\
-\sigma_g^*(\mathbf{x})\left[2\phi\left(\frac{e-\mu_g^*(\mathbf{x})}{\sigma_g^*(\mathbf{x})}\right) - \phi\left(\frac{e^- - \mu_g^*(\mathbf{x})}{\sigma_g^*(\mathbf{x})}\right) - \phi\left(\frac{e^+ - \mu_g^*(\mathbf{x})}{\sigma_g^*(\mathbf{x})}\right)\right] \\
+\delta\left[\Phi\left(\frac{e^+ - \mu_g^*(\mathbf{x})}{\sigma_g^*(\mathbf{x})}\right) - \Phi\left(\frac{e^- - \mu_g^*(\mathbf{x})}{\sigma_g^*(\mathbf{x})}\right)\right]
\end{aligned} \tag{13}
$$

where $e^- = e - \delta$, $e^+ = e + \delta$, in which e is the failure threshold, and δ is usually chosen by $\delta = 2\sigma_g^*(\mathbf{x})$. $\Phi(\cdot)$ and $\phi(\cdot)$ are the cumulative density function (CDF) and probability density function (PDF) of a standard normal random variable.

The process of AK-SYS and EGRA-SYS is as follows:

(1) Generate a small number of initial TPs, denoted by $\mathbf{x}_{kT}$; evaluate the limit-state functions $\mathbf{y}_{kT} = g_k(\mathbf{x}_{kT})$, where $k = 1, 2, ..., M$, and M is the number of components.

(2) Build surrogate models $\hat{y}_k = \hat{g}_k(\mathbf{x}_{kT})$.

(3) Generate Monte Carlo samples for input random variables $\mathbf{x}_{MCS}$.

(4) Evaluate the composite *U* function and *EFF* function at $\mathbf{x}_{MCS}$ using the predictions and standard deviations from $\hat{y}_k = \hat{g}_k(\mathbf{x}_{kT})$.

(5) Find the minimal value of the composite *U* learning function among those at all points in $\mathbf{x}_{MCS}$. For the EGRA method, find the maximal value of the composite *EFF* learning function among those at all points in $\mathbf{x}_{MCS}$.

(6) Check the convergence: The process converges if $U_{\min}^* \geq 2$ or $EFF_{\max}^* \leq 0.001$, and then perform reliability analysis using $\hat{y}_k = \hat{g}_k(\mathbf{x}_{kT})$; otherwise, go to Step (7).

(7) Identify a new TP $\mathbf{x}_{new}$ with the minimal composite learning function value $U^*_{\min}$ or the maximal composite learning function $EFF^*_{\max}$.

(8) Calculate the component U_k or EFF_k with high uncertainty at $\mathbf{x}_{new}$, and check $U_k < 2$ or $EFF_k > 0.001$.

(9) Add $\mathbf{x}_{new}$ and the responses at $\mathbf{x}_{new}$ to the existing training point set and update the surrogate models.

Repeat steps (2) through (9) till convergence.

As discussed previously, the larger is *U* or *EFF*, the higher is the chance that the Kriging model is accurate. In Step 8, the threshold of 2 is taken for *U* to check the convergence. The threshold of *EFF* is taken 0.001.

The size of $\mathbf{x}_{MCS}$ is determined by the estimate of the probability of system failure p_{sf} and the coefficient of variation COV_{psf}. The relationship is given by

$$COV_{psf} = \sqrt{\frac{1-p_{sf}}{p_{sf}N_{MCS}}} \tag{14}$$

where N_{MCS} is the size of $\mathbf{x}_{MCS}$. N_{MCS} may vary so that $COV_{psf} \le 5\%$.

Without the consideration of correlation, AK-SYS and EGRA-SYS use only mean predictions as shown in the following indicator function

$$I(\mathbf{x}) = \begin{cases} 1, & \mu^*_g(\mathbf{x}) < 0 \\ 0, & \text{otherwise} \end{cases} \tag{15}$$

Then p_f is estimated by

$$p_f = \frac{1}{N}\sum_{i=1}^{N} I(\mathbf{x}_i) \tag{16}$$

where N is the number of samples in $\mathbf{x}_{MCS}$.

2.3 Review of dependent Kriging method for component reliability

The dependent Kriging method (DKM) accounts for dependence between predictions to achieve better accuracy and efficiency. DKM uses all the information of the surrogate model $\hat{y} = \hat{g}(\mathbf{x}) = \mu(\mathbf{x}) + \varepsilon(\mathbf{x})$, where $\varepsilon(\mathbf{x}) \sim N(0, \sigma^2(\mathbf{x}))$ with correlation matrix $\mathbf{R}$. DKM computes p_f by

$$p_f = \int_{\mu(x)+\varepsilon(x)<0} f(\mathbf{x})d\mathbf{x} = \int I(\mathbf{x}) f(\mathbf{x})d\mathbf{x} = E[I(\mathbf{x})] \tag{17}$$

where $I(\cdot)$ is the indicator function defined by

$$I(x) = \begin{cases} 1, \ \hat{y} = \hat{g}(\mathbf{x}) = \mu(\mathbf{x}) + \varepsilon(\mathbf{x}) < 0 \\ 0, \ \text{otherwise} \end{cases} \tag{18}$$

p_f is a random variable since the domain of integration in Eq. (17) is random. The expectation of p_f is used to the estimate of the probability of failure [34]

$$E[p_f] = \frac{1}{N}\sum_{i=1}^{N} E(I_i) = \frac{1}{N}\sum_{i=1}^{N} e_i \tag{19}$$

where

$$e_i = \Phi(-\frac{\mu(\mathbf{x}_i)}{\sigma(\mathbf{x}_i)}) \tag{20}$$

The variance of p_f is used to estimate the error of p_f and is given by

$$Var(p_f) = \frac{1}{N^2}\sum_{i=1}^{N}[e_i(1-e_i) + \sum_{i=1, j\neq i}^{N}(e_{ij} - e_i e_j)] \tag{21}$$

where $e_{ij} = \Pr\{\hat{g}(\mathbf{x}_i) < 0, \hat{g}(\mathbf{x}_j) < 0\}$ is the CDF of the bivariate normal distribution defined by means $[\mu_i, \mu_j]$, standard deviations $[\sigma_i, \sigma_j]$, and correlation r_{ij}. Eq. (21) indicates that $Var(p_f)$

is the sum of N terms of the N sample points. Each term can be considered as the contribution from each sample. The contribution of one sample i is defined as the learning function below.

$$c_i = e_i(1-e_i) + \sum_{i=1, j\neq i}^{N} (e_{ij} - e_i e_j) \tag{22}$$

The learning function uses all the information of a Gaussian process, including its mean, variance, and correlation. As a result, it provides a more accurate and efficient way of selecting TPs to build surrogate models. In [34], selected candidate points (SCPs) are used to relieve the computational burden of the bivariate joint probability evaluation in Eq. (22). e_{ij} is not calculated for all points in $\mathbf{x}_{MCS}$, and a smaller number of points in $\mathbf{x}_{MCS}$ are selected to form the SCPs. Then the evaluations of e_{ij} is performed with only SCPs. The SCPs are selected based on two criteria. The first criterion is a small error in the estimate of p_f, and this criterion requires a significant number of points fall into the failure region. The second criterion is a high contribution to $Var(p_f)$. Therefore the SCPs consist of all the points in the failure region and other points with the highest indicator function variances in the safe region. Details of the implementation is given in [34].

3. DEPENDENT KRIGING METHOD FOR SYSTEM RELIABILITY

The new dependent Kriging method for systems (DKM-SYS) is the extension of component DKM to system reliability analysis. Similar to the component DKM, DKM-SYS consists of the same components: the estimate of probability of failure, a learning function, a stopping criterion, and an implementation process.

3.1 Estimate of p_{sf}

In this work, we consider a series system with k failure modes. For a series system, if at least one failure mode occurs, the system fails, and then the system reliability is computed by

$$R_s = \Pr\{g_1(\mathbf{x}) > 0 \bigcap g_2(\mathbf{x}) > 0 \bigcap ..... \bigcap g_k(\mathbf{x}) > 0\} \tag{23}$$

where $\bigcap$ denotes intersection. The safe region Ω is therefore defined by

$$\Omega = \{\mathbf{x} \mid g_1(\mathbf{x}) > 0 \bigcap g_2(\mathbf{x}) > 0 \bigcap ..... \bigcap g_k(\mathbf{x}) > 0\} \tag{24}$$

The system is safe at point **x** if **x** falls into Ω. Thus R_s is computed by

$$R_s = \int_{\Omega} f(\mathbf{x}) d\mathbf{x} = \int I_s(\mathbf{x}) f(\mathbf{x}) d\mathbf{x} = E[I_s(\mathbf{x})] \tag{25}$$

where the system indicator function is defined by

$$I_s(\mathbf{x}) = \begin{cases} 1, & \mathbf{x} \in \Omega \\ 0, & \text{otherwise} \end{cases} \tag{26}$$

R_s can be estimated by

$$R_s = \frac{1}{N} \sum_{i=1}^{N} I_s(\mathbf{x}_i) = \frac{1}{N} \sum_{i=1}^{N} I_{si} \tag{27}$$

where $I_{si} = I_s(\mathbf{x}_i)$. The system reliability at $\mathbf{x}_i \in \mathbf{x}_{MCS}$ is

$$\Pr\{I_{si} = 1\} = \Pr\{\hat{g}_1(\mathbf{x}_i) > 0 \bigcap \hat{g}_2(\mathbf{x}_i) > 0 \bigcap ..... \bigcap \hat{g}_k(\mathbf{x}_i) > 0\} \tag{28}$$

Thus, the probability of system failure at $\mathbf{x}_i \in \mathbf{x}_{MCS}$ is

$$p_{sf} = 1 - R_s = 1 - \frac{1}{N} \sum_{i=1}^{N} I_{si} \tag{29}$$

In this work, we generate surrogate models for limit-state functions separately and assume the predictions of the *k* responses at the same point are independent. (The responses of a single limit-state function at two points, however, are still dependent.) Thus, the joint probability density functions (PDF) of the *k* responses at point $\mathbf{x}_i$ are the product of their marginal PDFs. Eq. (28) is then rewritten as

$$\Pr\{I_{si}=1\}=\prod_{k=1}^{M}\Pr\{\hat{g}_k(\mathbf{x}_i)>0\} \tag{30}$$

At point $\mathbf{x}_i$, the reliability of component *k* is

$$\Pr\{\hat{g}_k(\mathbf{x}_i)>0\}=\Phi\left(\frac{\mu_k(\mathbf{x}_i)}{\sigma_k(\mathbf{x}_i)}\right)=r_{ki} \tag{31}$$

Thus

$$\Pr\{I_{si}=1\}=\prod_{k=1}^{M}r_{ki} \tag{32}$$

$$\Pr\{I_{si}=0\}=1-\prod_{k=1}^{M}r_{ki} \tag{33}$$

The expectation of the system indicator at $\mathbf{x}_i$ is

$$E[I_{si}]=1\cdot(\Pr\{I_{si}=1\})+0\cdot(\Pr\{I_{si}=0\})=\prod_{k=1}^{M}r_{ki} \tag{34}$$

The variance of the system indicator is

$$Var[I_{si}]=E[(I_{si})^2]-(E[I_{si}])^2=\prod_{k=1}^{M}r_{ki}-\left(\prod_{k=1}^{M}r_{ki}\right)^2=\left(1-\prod_{k=1}^{M}r_{ki}\right)\prod_{k=1}^{M}r_{ki} \tag{35}$$

Since R_s is a random variable, its expectation is used for the estimate of the system reliability; namely

$$E[R_s]=\frac{1}{N}\sum_{i=1}^{N}E[I_{Si}]=\frac{1}{N}\sum_{i=1}^{N}\left(\prod_{k=1}^{M}r_{ki}\right) \tag{36}$$

The probability of system failure p_{sf} is

$$E[p_{sf}]=1-\frac{1}{N}\sum_{i=1}^{N}\left(\prod_{k=1}^{M}r_{ki}\right) \tag{37}$$

The variance of p_{sf} is the same with the variance of R_s, which is calculated by

$$Var[p_{sf}] = Var[R_s] = \frac{1}{N^2} Var \sum_{i=1}^{N} I_{Si} = \frac{1}{N^2} [\sum_{i=1}^{N} Var[I_{si}] + 2 \sum_{i=1}^{N} \sum_{j>i}^{N} \text{cov}(I_{si}, I_{sj})] \tag{38}$$

$Var[p_{sf}]$ is determined by the covariance $\text{cov}(I_{si}, I_{sj})$, which is given by

$$\text{cov}(I_{si}, I_{sj}) = E[I_{si} I_{sj}] - E[I_{si}] E[I_{sj}] = \Pr\{I_{si} = 1, I_{sj} = 1\} - E[I_{si}] E[I_{sj}] \tag{39}$$

where

$$E[I_{si}] E[I_{sj}] = \prod_{k=1}^{M} r_{ki} \prod_{k=1}^{M} r_{kj} \tag{40}$$

Let $H = \Pr\{I_{si} = 1, I_{sj} = 1\}$, Eq. (38) becomes

$$Var[p_{sf}] = \frac{1}{N^2} \left\{ \sum_{i=1}^{N} \left[\left(1 - \prod_{k=1}^{M} r_{ki} \right) \prod_{k=1}^{M} r_{kj} \right] + 2 \sum_{i=1}^{N} \sum_{j>i}^{N} \left(H - \prod_{k=1}^{M} r_{ki} \prod_{k=1}^{M} r_{kj} \right) \right\} \tag{41}$$

where

$$H = \Pr\{I_{si} = 1, I_{sj} = 1\} = \Pr\{[\hat{g}_1(\mathbf{x}_i) > 0 \bigcap ... \bigcap \hat{g}_k(\mathbf{x}_i) > 0] \bigcap [\hat{g}_1(\mathbf{x}_j) > 0 \bigcap ... \bigcap \hat{g}_k(\mathbf{x}_j) > 0]\} \tag{42}$$

Eq. (42) is the probability of system safety at points $\mathbf{x}_i$ and $\mathbf{x}_j$. Since the predictions of all the responses are independent, H is given by

$$H = \Pr\{I_{si} = 1, I_{sj} = 1\} = \prod_{k=1}^{M} \Pr\{\hat{g}_{ki} > 0, \hat{g}_{kj} > 0\} = r_{kij} \tag{43}$$

where r_{kij} is the probability that component *k* is safe at point *i* and *j*.

Eq. (41) can be rewritten as

$$Var[p_{sf}] = \frac{1}{N^2} \sum_{i=1}^{N} \left\{ \left(1 - \prod_{k=1}^{M} r_{ki} \right) \prod_{k=1}^{M} r_{ki} + 2 \sum_{j=1, j \neq i}^{N} \left(\prod_{k=1}^{M} r_{kij} - \prod_{k=1}^{M} r_{ki} \prod_{k=1}^{M} r_{kj} \right) \right\} \tag{44}$$

or

$$Var[p_{sf}] = \frac{1}{N^2} \sum_{i=1}^{N} c_i \tag{45}$$

where

$$c_i = \frac{1}{N^2}\sum_{i=1}^{N}\left\{\left(1-\prod_{k=1}^{M} r_{ki}\right)\prod_{k=1}^{M} r_{ki} + 2\sum_{j=1, j\neq i}^{N}\left(\prod_{k=1}^{M} r_{kij} - \prod_{k=1}^{M} r_{ki}\prod_{k=1}^{M} r_{kj}\right)\right\} \tag{46}$$

Therefore, the standard deviation of p_{sf} is

$$\sigma_{p_{sf}} = \frac{1}{N}\sqrt{\sum_{i=1}^{N} c_i} \tag{47}$$

$\sigma_{p_{sf}}$ is an indicator of the uncertainty associated with the estimate of the system reliability. If there was no model uncertainty, $\sigma_{p_{sf}}$ would be zero. The higher $\sigma_{p_{sf}}$ is, the higher the uncertainty associated with the system reliability estimated based on the surrogate models is. We therefore use $\sigma_{p_{sf}}$ to measure the error of the system reliability prediction.

3.2 Learning function

A learning function is used to select new TPs to refine the surrogate model. As indicated in Eq. (44), each TP contributes to $\sigma_{p_{sf}}$ or $Var[p_{sf}]$. The sum of terms involving $\mathbf{x}_i$ in $Var[p_{sf}]$ is c_i in Eq. (46). Thus, we use c_i as the learning function. Maximizing c_i identifies a new TP that has the highest contribution to the uncertainty of the estimate of system reliability; namely

$$\begin{cases} \mathbf{x}_{new} = \mathbf{x}_h \\ h = \arg\max_{i=1,2,\ldots,N_{MCS}} \{c_i\} \end{cases} \tag{48}$$

where $\mathbf{x}_h$ is the h-th point in $\mathbf{x}_{MCS}$. Adding the highest contribution point as new TP is the most effective way to refine the surrogate model with fast convergence [34].

3.3 Stopping criterion

When $\sigma_{p_{sf}}$ is small enough, no more new TPs are needed. Then the surrogate models are used to calculate p_{sf}. Let the confidence of the probability of system failure be $1-\alpha$ and the allowable relative error be ε, and then the confidence interval of the estimate is computed by $E[p_{sf}]\pm\Phi(\alpha/2)\sigma_{p_{sf}}$.

The relative error is defined by

$$\eta=\frac{\left|E[p_{sf}]\pm\Phi^{-1}(\alpha/2)\sigma_{p_{sf}}-E[p_{sf}]\right|}{E[p_{sf}]}=\left|\frac{\Phi^{-1}(\alpha/2)\sigma_{p_{sf}}}{E[p_{sf}]}\right| \tag{49}$$

If η is smaller than the allowable error, the process terminates. Thus, the stopping criterion is determined by

$$\frac{\sigma_{p_{sf}}}{E[p_{sf}]}\le\left|\frac{\eta}{\Phi^{-1}(\alpha/2)}\right| \tag{50}$$

3.4 Implementation

Accounting for the dependence between responses requires calculations of bivariate probabilities given by

$$r_{kij}=\Pr\{g_{ki}>0,g_{kj}>0\},(k=1,..M;i,j=1,2,\cdots,N,i\neq j) \tag{51}$$

Calculating r_{kij} is time consuming. For example, if the size of $\mathbf{x}_{MCS}$ is 10^5, the number of calculating the joint probability in r_{kij} is $\frac{N(1+N)}{2}=\frac{10^5(1+10^5)}{2}\approx1.5\times10^{10}$. To relieve the computational burden, we use the so-called selected candidate points (SCPs), denoted by $\mathbf{x}_S$, which are selected from $\mathbf{x}_{MCS}$. The size of $\mathbf{x}_S$ is much smaller than that of $\mathbf{x}_{MCS}$. To ensure a

significant number of points fall into the failure region, we adjust the size of SCPs N_{sel} using the following condition.

$$25\% \le r = \frac{N_{F,sel}}{N_{sel}} \le 75\% \tag{52}$$

where $N_{F,Sel}$ is the number of failure points in the SCPs. SCPs consist of all points in the failure region and the other points with highest indicator function variances in the safe region. Using SCPs, the computational effort needed is greatly reduced. In the examples in Sec.4, we use 200 SCPs.

The stopping criterion in Eq. (50) needs to be modified accordingly. The probability of system failure using $\mathbf{x}_S$ is calculated by

$$E[p_{sf,sel}] = 1 - \frac{1}{N_{sel}} \sum_{i=1}^{N_{sel}} r_i \tag{53}$$

and

$$\sigma_{Psf,sel} = \frac{1}{N_{sel}} \sqrt{\sum_{i=1}^{N_{sel}} c_i} \tag{54}$$

The stopping criterion becomes

$$\frac{\sigma_{P_{sf},sel}}{E[p_{sf,sel}]} \le \left| \frac{\eta}{\Phi^{-1}(\alpha/2)} \right| \tag{55}$$

The flowchart of the DKM-SYS is provided below.

Place Figure 1 here

Fig.1 Flowchart of DKM-SYS

3.5 Parallel systems

The above results can be extended to parallel systems. For a parallel system with k failure modes, the probability of failure can be computed by

$$p_{fs} = \Pr\{g_1(\mathbf{x}) < 0 \bigcap g_2(\mathbf{x}) < 0 \bigcap ..... \bigcap g_k(\mathbf{x}) < 0\} \tag{56}$$

Let $G_i(\mathbf{x}) = -g_i(\mathbf{x})$, then

$$p_{fs} = \Pr\{G_1(\mathbf{x}) > 0 \bigcap G_2(\mathbf{x}) > 0 \bigcap ..... \bigcap G_k(\mathbf{x}) > 0\} \tag{57}$$

Eq. (57) evaluates the probability of a union of n-events as Eq. (23) does. Hence the proposed method can be used to calculate Eq. (57), which leads to the parallel system reliability $R_s = 1 - p_{fs}$.

4. EXAMPLES

The proposed method is evaluated with four examples. The first example is a mathematical problem, which clearly demonstrates the application details and effectiveness of DKM-SYS, while the other three examples show possible engineering applications.

In all examples, initial TPs are generated by the Latin hypercube sampling (LHS) [35], and the initial sample size is 12. The efficiency is measured by the number of limit-state function calls. The accuracy is measured by the percentage error with respect to the direct MCS. The error is calculated by

$$\varepsilon = \frac{\left| p_{sf} - p_{sf}^{MCS} \right|}{p_{sf}^{MCS}} \times 100\% \tag{58}$$

where p_{sf}^{MCS} and p_{sf} are probabilities of system failure from the direct MCS and the other method, respectively. Since Kriging-based reliability methods are stochastic methods, we run each method 20 independently, and the average results are used for comparison. The standard deviation of the number of function calls and probabilities of system failure are also provided. A smaller standard

deviation means that the results are concentrated closer to their mean values, which indicates that the method tends to produce more stable results. We therefore use the standard deviation as an indicator of the robustness of the method.

4.1 Example 1

This example involves two random variables and three mathematical equations. For this two-dimensional problem, it is easy to demonstrate the effectiveness of the proposed method. The three limit-state functions are given by [36]

$$g_1(\mathbf{x}) = (x_2^2 + 11)(x_1 - 1)/5 - \cos(3x_2) - 5 \tag{59}$$

$$g_2(\mathbf{x}) = (x_1 + x_2 - 5)^2/30 + (x_1 - x_2 - 12)^2/120 - 1 - \cos(3x_1)/10 \tag{60}$$

$$g_3(\mathbf{x}) = 80/(x_1^2 + 8x_2 - 5) - \cos(3x_2)/10 - 1 \tag{61}$$

where $x_i \sim N(4, 0.7^2)$, $i = 1, 2$. Figs. 2 and 3 show the TPs and surrogate models using AK-SYS and DKM-SYS method, respectively.

Place Figure 2 here

(a) Training points (b) Final surrogate models

Fig. 2 Training points and surrogate models of AK-SYS

Place Figure 3 here

(a) Training points (b) Final surrogate models

Fig. 3 Training points and surrogate models of DKM-SYS

The average numbers of function calls and the average probabilities of system reliability based on direct MCS and LHS are provided in Table 1 and Table 2, respectively. The difference of results from the two sampling methods is not significant since the sample size is large. For this reason, we compare two different sampling methods for only this example.

We also compare the probabilities of system failure from DKM-SYS, AK-SYS and EGRA-SYS with those from the direct MCS and LHS. In both tables, the results show that DKM-SYS is more accurate than AK-SYS and EGRA-SYS. DKM-SYS is also more efficient than AK-SYS and DKM-SYS since the former method has smaller average numbers of function calls. Limit-state function 3 is far away from the origin as shown in Figs. 2 and 3, and it is hard to obtain an accurate surrogate model. This function consumes the majority of the computational effort by DKM-SYS, AK-SYS and EGRA-SYS.

Table 1 Average results from 20 runs based on direct MCS

Place Table 1 here

Table 2 Average results from 20 runs based on Latin hypercube sampling

---

Place Table 2 here

4.2 Exmaple 2

This is an engineering problem with a small probability of system failure. This problem involves a liquid hydrogen fuel tank that is used on a space launch vehicle [31, 37, 38]. The tank has a honeycomb sandwich deign. It is subjected to stress caused by ullage pressure, head pressure, axial force due to acceleration, and bending and shear stress due to the weight of the fuel. There are three failure modes related to the von Mises strength, isotropic strength, and honeycomb bucking. The limit-state functions for the von Mises and isotropic strength are given by

$$g_1(\mathbf{X}) = \frac{84000 t_{plate}}{\sqrt{N_x^2 + N_y^2 - N_x N_y + 3N_{xy}^2}} - 1 \tag{62}$$

$$g_2(\mathbf{X}) = \frac{84000 t_{plate}}{\left|N_y\right|} - 1 \tag{63}$$

The limit-state function of honeycomb buckling is defined by a response surface generated from the structural sizing program and is given by [31, 38].

$$\begin{aligned} g_3(\mathbf{X}) &= 0.847 + 0.96 y_1 + 0.986 y_2 - 0.216 y_3 + 0.077 y_1^2 \\ &+ 0.11 y_2^2 + 0.007 y_3^2 + 0.378 y_1 y_2 - 0.106 y_1 y_3 - 0.11 y_2 y_3 \end{aligned} \tag{64}$$

where

$$y_1 = 4(t_{plate} - 0.075) \tag{65}$$

$$y_2 = 20(t_h - 0.1) \tag{66}$$

$$y_3 = -6000\left(\frac{1}{N_{xy}} + 0.003\right) \tag{67}$$

The five independent random variables are given in Table 3. The reliability analysis results are provided in Table 4.

Table 3 Random variables

Place Table 3 here

Table 4 shows that the average total function call of AK-SYS and EGRA-SYS are 56.1 and 43.35 respectively, while the average total function call of DKM-SYS is 42.45. This demonstrates that DKM-SYS is more efficient. DKM-SYS is also more accurate than AK-SYS and EGRA-SYS, because the error of DKM-SYS is only 0.57% and the errors of the other two methods are relatively large.

Table 4 Comparison of average results from 20 runs

Place Table 4 here

4.3 Example 3

This is an engineering problem that involves a relatively large set of input random variables. As shown in Fig. 4, a cantilever beam [39] with ten random variables is used to prove the robustness of DKM-SYS method.

The beam is subjected to external forces F_1 and F_2, external moments M_1 and M_2, and external distributed loads denoted by (q_{L1}, q_{R1}) and (q_{L2}, q_{R2}). These forces, moments, distributed loads, together with the yield strength S and the maximum allowable shear stress $\tau_{\max}$ are normally distributed random variables. Their information is given in Table 5. The deterministic parameters are listed in Table 6.

Place Figure 4 here

Fig.4 A cantilever beam

Table 5 Random variables

Place Table 5 here

Table 6 Deterministic parameters

Place Table 6 here

The maximum normal stress of the beam should be smaller than its yield strength, and this is given by

$$g_1(\mathbf{X}) = S - \frac{6M}{wh^2} \tag{68}$$

where the bending moment at the left end point of the beam is

$$M = \sum_{i=1}^{2} M_i + \sum_{i=1}^{2} F_i b_i + \sum_{i=1}^{2} \frac{q_{Li}(d_i - c_i)(d_i + c_i)}{2} + \sum_{i=1}^{2} \frac{(q_{Ri} - q_{Li})(d_i - c_i)(2d_i + c_i)}{6} \tag{69}$$

The deflection of the right end point of the beam should not greater than the allowable defection $\delta_{allowable} = 2$ cm.

$$g_2(\mathbf{X}) = \delta - \delta_{allowable} \tag{70}$$

where δ is computed by

$$\delta = \frac{1}{EI}[\frac{ML^2}{2} + \frac{PL^3}{6} + \sum_{i=1}^{2}\frac{M_i(L-a_i)^2}{2} - \sum_{i=1}^{2}\frac{F_i(L-b_i)^3}{6} - \sum_{i=1}^{2}\frac{q_{Li}(L-c_i)^4}{24} - \sum_{i=1}^{2}\frac{(q_{Ri}-q_{Li})(L-c_i)^5}{120(d_i-c_i)} + \sum_{i=1}^{2}\frac{q_{Ri}(L-d_i)^4}{24} + \sum_{i=1}^{2}\frac{(q_{Ri}-q_{Li})(L-d_i)^5}{120(d_i-c_i)}] \quad (71)$$

where the Young's modulus is $E = 2\times10^{11}$ Pa, and the moment of inertia is $I = wh^3/12$. P is the reaction force at the fixed end, which is given by

$$P = \sum_{i=1}^{2}F_i + \sum_{i=1}^{2}q_{Li}(d_i - c_i) + \sum_{i=1}^{2}\frac{(q_{Ri}-q_{Li})(d_i-c_i)}{2} \quad (72)$$

The last limit-state function specifies that the shear stress should not be greater than the maximum allowable shear stress

$$g_3(\mathbf{X}) = \tau_{\max} - \tau = \tau_{\max} - \frac{3P}{2wh} \quad (73)$$

The results from Table 7 also show that DKM-SYS has better performance than AK-SYS and EGRA-SYS in accuracy, efficiency. The significant advantage of DKM-SYS over AK-SYS and EGRA-SYS in this example is the efficiency. On average, the total function calls of AK-SYS and EGRA-SYS are 353.64 and 477, while DKM-SYS just needs 129.5 function calls.

Table 7 Comparison of average results from 20 runs

Place Table 7 here

4.4 Example 4

This problem involves more failure modes than the previous examples. A crank-slider system is considered which has four components shown in Fig. 5 [40]. An external moment is applied to

joint A to drive link AB rotating around A. The task is to predict the system reliability when $\theta_2 = \pi / 2$ and five failure modes are considered for this system.

Place Figure 5 here

Fig. 5 A crank-slider system

For link AB, the length is l_1, and the width and height of the cross section are b_1 and h_1. The maximal normal stress $S_1 = \dfrac{M(h_1/2)}{b_1 h_1^3/12}$ developed in the link AB should be smaller than the allowable normal stress S_{a1} and this is given by

$$g_1(\mathbf{X}) = S_{a1} - S_1 \tag{74}$$

For link BC, the length is l_2, and the width and height of the cross section are b_2 and h_2. The force developed in the link F_{BC} should be smaller than the critical force for buckling P_{cr}.

$$g_2(\mathbf{X}) = P_{cr} - F_{BC} \tag{75}$$

where $F_{BC} = M / l_1$, $P_{cr} = \dfrac{\pi^2 E_2 I_2}{(K l_2)^2}$ and $I_2 = \dfrac{b_2 h_2^3}{12}$.

For shaft DE, the length and diameter are l_3 and d_4. It has two failure modes caused by excessive deflection and excessive normal stress, respectively. The corresponding limit-state functions are given by

$$\begin{cases} g_3(\mathbf{X}) = \delta_{a3} - \delta_3 \\ g_4(\mathbf{X}) = S_{a4} - S_4 \end{cases} \tag{76}$$

where δ_{a3} is the allowable deflection, and δ_3 is the maximal deflection given by

$$\delta_3 = \frac{F_{BC}\sin\left(\pi/2-\theta_1\right)l_4(l_3{}^2-l_4^2)^{3/2}}{9\sqrt{3}\ l_3E_4(\pi/4)(d_4/2)^4} \tag{77}$$

where E_4 is the Young's modulus of shaft DE. S_{a4} is the allowable normal stress, and S_4 is the maximal normal stress developed in the shaft and is calculated by

$$S_4 = \frac{M_{\max}c}{I_4} = \frac{F_{BC}\sin\left(\pi/2-\theta_1\right)(l_3-l_4)(d_4/2)}{(\pi/4)(d_4/2)^4} \tag{78}$$

For spring DE, the outer diameter and inner diameter of the spring are *D* and *d*. The developed maximal shear stress τ_5 should not be greater than the allowable shear stress of the spring coils τ_{a5}.

$$g_5(\mathbf{X}) = \tau_{a5} - \tau_5 \tag{79}$$

where τ_5 is computed by

$$\tau_5 = \frac{F_{BC}\cos\left(\pi/2-\theta_1\right)D}{\pi d^3}\left(\frac{4D-d}{4D-4d}+\frac{0.615d}{D}\right) \tag{80}$$

All the random variables are listed in Table 8, and the deterministic parameters are listed in Table 9. The reliability analysis results are provided in Table 10.

Table 8 Random variables

Place Table 8 here

Table 9 Deterministic parameter

Place Table 9 here

Table 10 Comparison of average results from 20 runs

Place Table 10 here

Table 10 shows the comparison between AK-SYS, EGRA-SYS, DKM-SYS, and MCS. It is obvious that DKM-SYS can achieve better accuracy and efficiency than AK-SYS and EGRA-SYS. In particular, the total average function call of DKM-SYS is 193.7, while that of AK-SYS and EGRA-SYS are 466.4 and 658.8, respectively.

5. CONCLUSIONS

This work develops a new system reliability method for series systems with multiple dependent failure modes using the Kriging method. High efficiency and accuracy are achieved through the following means: 1) the use of surrogate models from Kriging, 2) the use of all information from Kriging, such as the prediction and its standard deviation, in the estimate of the system reliability, and 3) an efficient way for selecting training points for refining surrogate models. Since the dependence between Kriging predictions at different points are considered and the error of system reliability estimate is directly quantified (instead of the error of surrogate models), the new method improves the performance of Kriging-based system reliability methods.

The proposed method extends the Kriging method from component reliability analysis to system reliability in an efficient manner. It can be potentially used for system reliability-based design and robust system design.

ACKNOWLEDGEMENTS

The authors gratefully acknowledge the support from the National Science Foundation through grants CMMI 1924413 and CMMI 1923799.

REFERENCES

[1] Singh, A., Mourelatos, Z. P., and Li, J., 2010, "Design for Lifecycle Cost Using Time-Dependent Reliability," Journal of Mechanical Design, 132(9), pp. 091008-091008-091011.
[2] Hu, Z., and Du, X., 2014, "Lifetime cost optimization with time-dependent reliability," Engineering Optimization, 46(10), pp. 1389-1410.
[3] Lee, I., Choi, K. K., and Gorsich, D., 2010, "Sensitivity analyses of FORM-based and DRM-based performance measure approach (PMA) for reliability-based design optimization (RBDO)," International Journal for Numerical Methods in Engineering, 82(1), pp. 26-46.
[4] Du, X., and Hu, Z., 2012, "First Order Reliability Method With Truncated Random Variables," Journal of Mechanical Design, 134(9), pp. 091005.
[5] Zhu, Z., Hu, Z., and Du, X., 2015, "Reliability Analysis for Multidisciplinary Systems Involving Stationary Stochastic Processes," Proceedings of the IDETC/CIE, ASME Paper, No. DETC2015-46168.
[6] Ditlevsen, O., and Madsen, H. O., 1996, Structural reliability methods, Wiley, Chichester; New York.
[7] Zio, E., 2013, System Reliability and Risk Analysis, Springer, London.
[8] Balesdent, M., Morio, J., and Marzat, J., 2013, "Kriging-based adaptive Importance Sampling algorithms for rare event estimation," Structural Safety, 44, pp. 1-10.
[9] Dubourg, V., Sudret, B., and Deheeger, F., 2013, "Metamodel-based importance sampling for structural reliability analysis," Probabilistic Engineering Mechanics, 33, pp. 47-57.
[10] Echard, B., Gayton, N., Lemaire, M., and Relun, N., 2013, "A combined Importance Sampling and Kriging reliability method for small failure probabilities with time-demanding numerical models," Reliability Engineering & System Safety, 111, pp. 232-240.
[11] Wang, Z., and Wang, P., 2015, "An Integrated Performance Measure Approach for System Reliability Analysis," Journal of Mechanical Design, 137(2), pp. 021406-021406-021411.
[12] Helton, J. C., Johnson, J. D., Sallaberry, C. J., and Storlie, C. B., 2006, "Survey of sampling-based methods for uncertainty and sensitivity analysis," Reliability Engineering & System Safety, 91(10), pp. 1175-1209.
[13] Hurtado, J. E., and Barbat, A. H., 1998, "Monte Carlo techniques in computational stochastic mechanics," Archives of Computational Methods in Engineering, 5(1), pp. 3.
[14] Viana, F. A.., Simpson, T. W., Balabanov, V., and Toropov, V., 2014, "Special Section on Multidisciplinary Design Optimization: Metamodeling in Multidisciplinary Design Optimization: How Far Have We Really Come?," AIAA Journal, 52(4), pp. 670-690.
[15] Picheny, V., 2009, "Improving accuracy and compensating for uncertainty in surrogate modeling," Ph.D. dissertation, University of Florida, Gainesville, FL.
[16] Sacks, J., Welch, W. J., Mitchell, T. J., and Wynn, H. P., 1989, "Design and Analysis of Computer Experiments," Statistical Science, 4(4), pp. 409-423.

[17] Youn, B. D., and Choi, K. K., 2004, "A new response surface methodology for reliability-based design optimization," Computers & Structures, 82(2), pp. 241-256.
[18] Bucher, C. G., and Bourgund, U., 1990, "A fast and efficient response surface approach for structural reliability problems," Structural Safety, 7(1), pp. 57-66.
[19]Hurtado, J. E., Alvarez, D. A., 2001, "Neural-network-based reliability analysis: a comparative study," Computer methods in applied mechanics and engineering, 191(1-2), pp. 113-132.
[20] Elhewy, A. H., Mesbahi, E., and Pu, Y., 2006, "Reliability analysis of structures using neural network method," Probabilistic Engineering Mechanics, 21(1), pp. 44-53.
[21] Xiao, N.-C., Zuo, M. J., and Zhou, C., 2018, "A new adaptive sequential sampling method to construct surrogate models for efficient reliability analysis," Reliability Engineering & System Safety, 169, pp. 330-338.
[22] Basudhar, A., Dribusch, C., Lacaze, S., Missoum, S., 2012, "Constrained efficient global optimization with support vector machines," Structural and Multidisciplinary Optimization, 46(2), pp. 201-221.
[23] Bourinet, J. M., Deheeger, F., and Lemaire, M., 2011, "Assessing small failure probabilities by combined subset simulation and Support Vector Machines," Structural Safety, 33(6), pp. 343-353.
[24] Basudhar, A., Missoum, S., and Safety, 2013, "Reliability assessment using probabilistic support vector machines," International Journal of Reliability and Safety, 7(2), pp. 156-173.
[25] Schöbi, R., Sudret, B., and Marelli, S., 2017, "Rare Event Estimation Using Polynomial-Chaos Kriging," ASCE-ASME Journal of Risk and Uncertainty in Engineering Systems, Part A: Civil Engineering, 3(2), pp. D4016002.
[26] Lophaven, S. N., Nielsen, H. B., and Sondergaard, J., 2002, "DACE-A Matlab Kriging toolbox, version 2.0," Technical University of Denmark, Lyngby, Denmark.
[27] Martin, J. D., and Simpson, T. W., 2005, "Use of Kriging Models to Approximate Deterministic Computer Models," AIAA Journal, 43(4), pp. 853-863.
[28] Kleijnen, J. P., "Design and Analysis of Simulation Experiments," Springer International Publishing, pp. 3-22.
[29] Jones, D. R., Schonlau, M., and Welch, W. J., 1998, "Efficient global optimization of expensive black-box functions," Journal of Global optimization, 13(4), pp. 455-492.
[30] Bichon, B. J., Eldred, M. S., Swiler, L. P., Mahadevan, S., and Mcfarland, J. M., 2012, "Efficient Global Reliability Analysis for Nonlinear Implicit Performance Functions," AIAA Journal, 46(10), pp. 2459-2468.
[31] Bichon, B. J., McFarland, J. M., and Mahadevan, S., 2011, "Efficient surrogate models for reliability analysis of systems with multiple failure modes," Reliability Engineering & System Safety, 96(10), pp. 1386-1395.
[32] Echard, B., Gayton, N., and Lemaire, M., 2011, "AK-MCS: An active learning reliability method combining Kriging and Monte Carlo Simulation," Structural Safety, 33(2), pp. 145-154.
[33] Fauriat, W., and Gayton, N., 2014, "AK-SYS: An adaptation of the AK-MCS method for system reliability," Reliability Engineering & System Safety, 123, pp. 137-144.
[34] Zhu, Z., and Du, X., 2016, "Reliability Analysis With Monte Carlo Simulation and Dependent Kriging Predictions," Journal of Mechanical Design, 138(12), pp. 121403-121403-121411.
[35] Viana, F. A. C., Venter, G., and Balabanov, V., 2010, "An algorithm for fast optimal Latin hypercube design of experiments," International Journal for Numerical Methods in Engineering, 82(2), pp. 135-156.

[36] Sadoughi, M., Li, M., and Hu, C., 2018, "Multivariate system reliability analysis considering highly nonlinear and dependent safety events," Reliability Engineering & System Safety, 180, pp. 189-200.
[37] McDonald, M., and Mahadevan, S., 2008, "Design Optimization With System-Level Reliability Constraints," Journal of Mechanical Design, 130(2), pp. 021403-021403-021410.
[38] Smith, N., and Mahadevan, S., 2005, "Integrating System-Level and Component-Level Designs Under Uncertainty," Journal of Spacecraft and Rockets, 42(4), pp. 752-760.
[39] Du, X., 2010, "System reliability analysis with saddlepoint approximation," Structural and Multidisciplinary Optimization, 42(2), pp. 193-208.
[40] Hu, Z., and Du, X., 2018, "Integration of Statistics- and Physics-Based Methods—A Feasibility Study on Accurate System Reliability Prediction," Journal of Mechanical Design, 140(7), pp. 074501-074501-074507.

List of Table Captions

List of Figure Captions

Table 1 Average results from 20 runs based on direct MCS

Method	p_{sf}	ε (%)	Number of function calls		
			N_1	N_2	N_3
AK-SYS	2.7249×10^{-2}	1.94	25.30	28.20	30.60
EGRA-SYS	2.7241×10^{-2}	1.97	26.05	29	32.05
DKM-SYS	2.7403×10^{-2}	1.37	17.85	22.25	22.45
MCS	2.750×10^{-2}	N/A	5×10^{6}	5×10^{6}	5×10^{6}

Table 2 Average results from 20 runs based on Latin hypercube sampling

Method	p_{sf}	ε (%)	Number of function calls		
			N_1	N_2	N_3
AK-SYS	2.7389×10^{-2}	1.24	25.5	28.5	30.0
EGRA-SYS	2.7472×10^{-2}	1.26	26.4	28.7	29.4
DKM-SYS	2.7403×10^{-2}	1.23	18.8	22.6	23.6
LHS	2.7474×10^{-2}	N/A	5×10^{6}	5×10^{6}	5×10^{6}

Table 3 Random variables

	Random variables	Distribution
X_1	t_{plate}	$\mathrm{N}(0.07433, 0.005)$
X_2	t_h	$\mathrm{N}(0.1, 0.01)$
X_3	N_x	$\mathrm{N}(13, 60)$
X_4	N_y	$\mathrm{N}(4751, 48)$
X_5	N_{xy}	$\mathrm{N}(-684, 11)$

Table 4 Comparison of average results from 20 runs

Method	p_{sf}	ε (%)	Number of function calls		
			N_1	N_2	N_3
AK-SYS	6.9756×10^{-4}	1.52	12	31.50	12.60
EGRA-SYS	6.9603×10^{-4}	2.01	12	18.10	13.25
DKM-SYS	7.0107×10^{-4}	0.57	12	19.10	12.40
MCS	6.9855×10^{-4}	N/A	2×10^{7}	2×10^{7}	2×10^{7}

Table 5 Random variables

	Random Variables	Distribution
X_1	M_1(Nm)	$\mathrm{N}(50\times10^3, 5\times10^3)$
X_2	M_2(Nm)	$\mathrm{N}(30\times10^3, 3\times10^3)$
X_3	F_1(m)	$\mathrm{N}(1.8\times10^4, 2\times10^3)$
X_4	F_2(m)	$\mathrm{N}(3\times10^4, 3\times10^3)$
X_5	q_{L1}(N/m)	$\mathrm{N}(3\times10^4, 1\times10^3)$
X_6	q_{R1}(N/m)	$\mathrm{N}(2\times10^4, 1\times10^3)$
X_7	q_{L2}(N/m)	$\mathrm{N}(2\times10^4, 1\times10^3)$
X_8	q_{R2}(N/m)	$\mathrm{N}(1\times10^3, 10)$
X_9	S(Pa)	$\mathrm{N}(4.5\times10^7, 4.5\times10^6)$
X_{10}	$\tau_{\max}$(Pa)	$\mathrm{N}(3.5\times10^6, 5\times10^5)$

Table 6 Deterministic parameters

Parameters	Values
a_1(m)	1.5
a_2(m)	4.5
b_1(m)	0.75
b_2(m)	2.5
c_1(m)	0.25
c_2(m)	1.75
d_1(m)	1.25
d_2(m)	4.75
L(m)	5
w(m)	0.2
h(m)	0.4

Table 7 Comparison of average results from 20 runs

Method	p_{sf}	ε(%)	Number of function calls		
			N_1	N_2	N_3
AK-SYS	5.2592×10^{-3}	1.74	245.89	12	95.75
EGRA-SYS	5.2542×10^{-3}	1.71	355	15	107
DKM-SYS	5.2657×10^{-3}	0.94	70.80	13.05	45.65
MCS	5.2567×10^{-3}	N/A	1×10^{7}	1×10^{7}	1×10^{7}

Table 8 Random variables

	Random Variables	Distribution
X_1	M_1(Nm)	N(350, 65)
X_2	l_1(m)	N(0.3, 10^{-4})
X_3	l_2(m)	N(0.9, 2×10^{-3})
X_4	b_1(m)	N(0.022, 5×10^{-4})
X_5	h_1(m)	N(0.019, 5×10^{-4})
X_6	b_2(m)	N(0.015, 5×10^{-4})
X_7	h_2(m)	N(0.009, 5×10^{-4})
X_8	d_4(m)	N(0.0228, 1×10^{-4})
X_9	D(m)	N(34.7×10^{-3}, 1×10^{-4})
X_{10}	τ_{a5}(m)	N(50×10^{6}, 10×10^{6})

Table 9 Deterministic parameter

Deterministic Parameters	Values
E_2(Pa)	200×10^9
E_4(Pa)	200×10^9
K	1
l_3(m)	0.95
l_4(m)	0.30
S_{a1}(Pa)	400×10^6
S_{a4}(Pa)	460×10^6
δ_{a3}(m)	0.0053
d(m)	29.5×10^{-3}

Table 10 Comparison of average results from 20 runs

Method	p_{sf}	ε (%)	Number of function calls				
			N_1	N_2	N_3	N_4	N_5
AK-SYS	1.3638×10^{-2}	1.92	149.95	215	12	12	77.45
EGRA-SYS	1.3655×10^{-2}	1.91	214.75	303.70	12	17.40	110.95
DKM-SYS	1.3713×10^{-2}	0.81	54.35	76.25	12.05	12.15	38.90
MCS	1.3643×10^{-2}	N/A	5×10^{6}	5×10^{6}	5×10^{6}	5×10^{6}	5×10^{6}

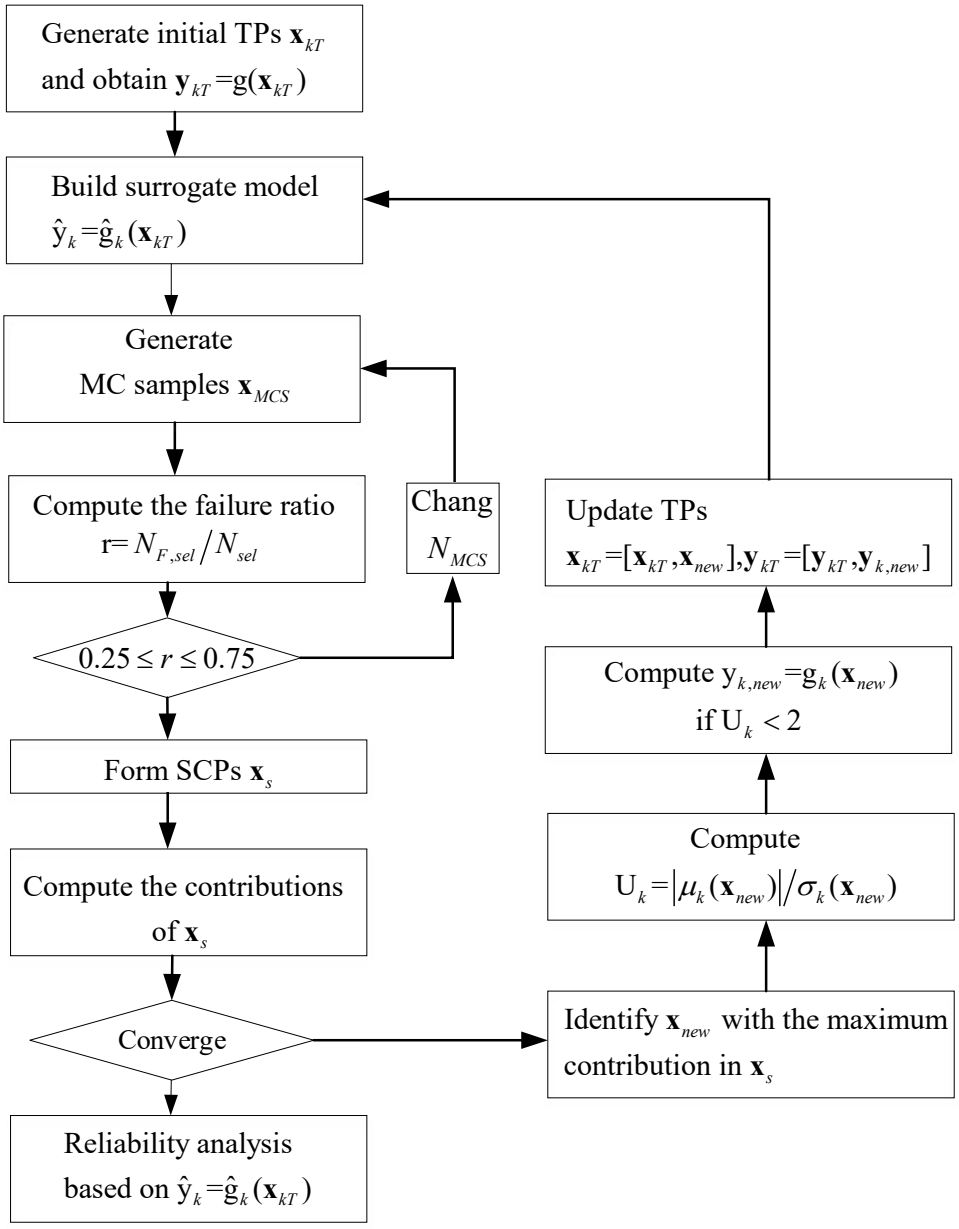

Fig.1 Flowchart of DKM-SYS

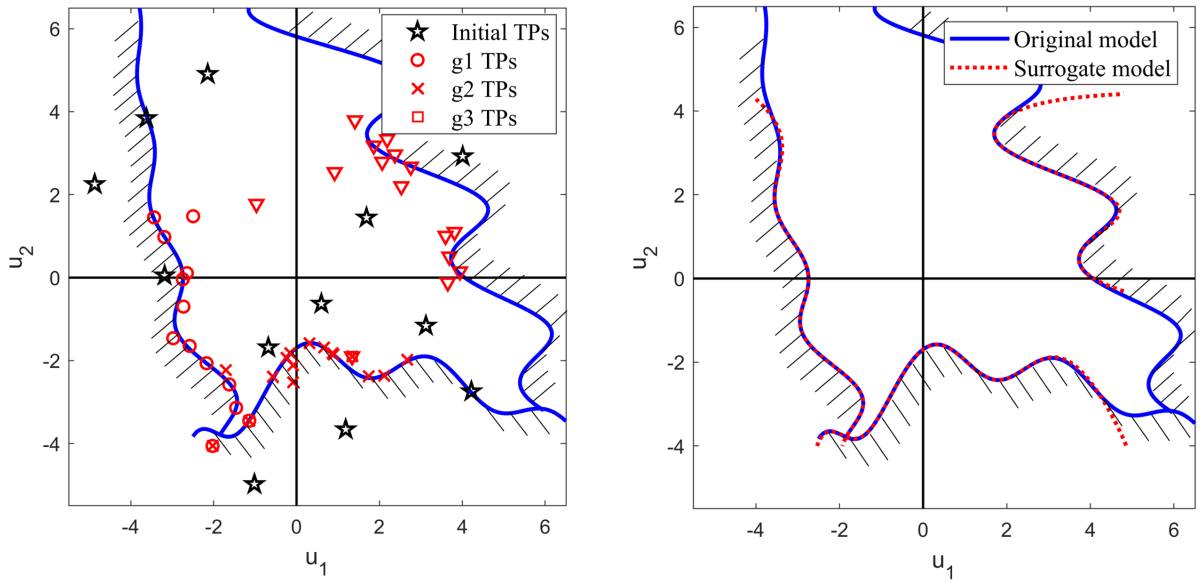

Fig. 2 Training points and surrogate models of AK-SYS

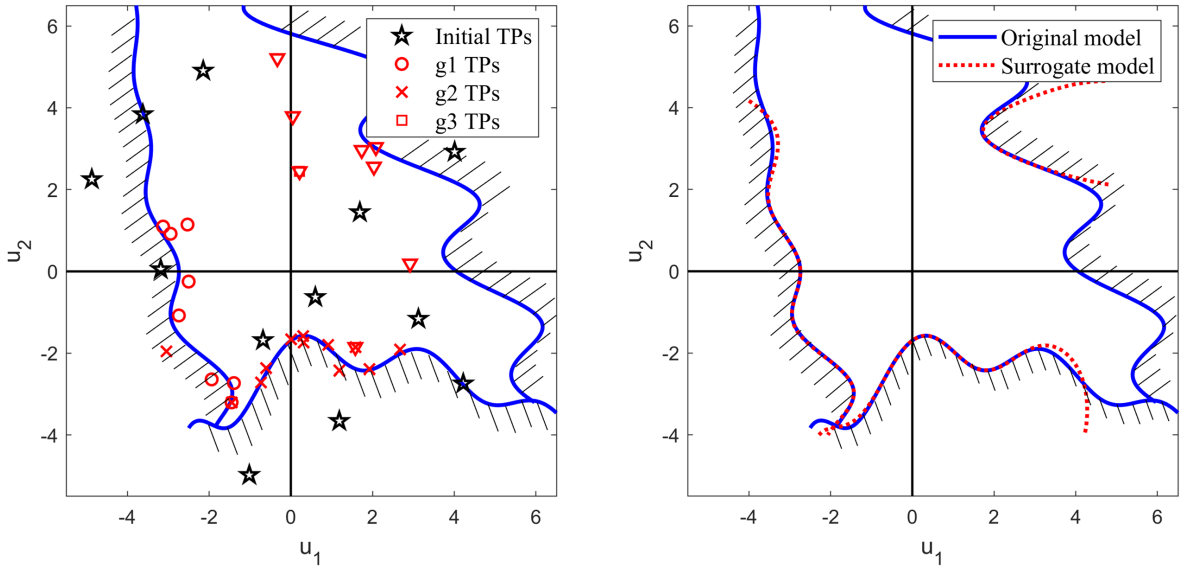

Fig. 3 Training points and surrogate models of DKM-SYS

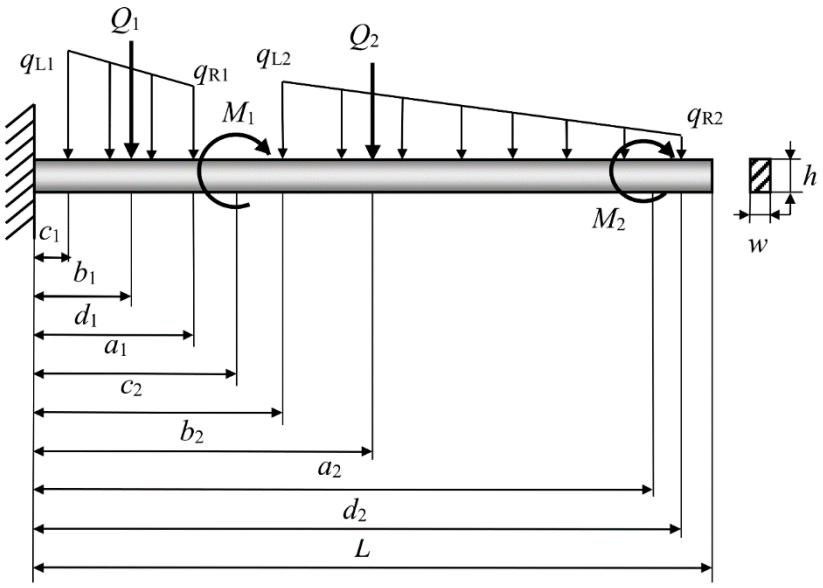

Fig.4 A cantilever beam

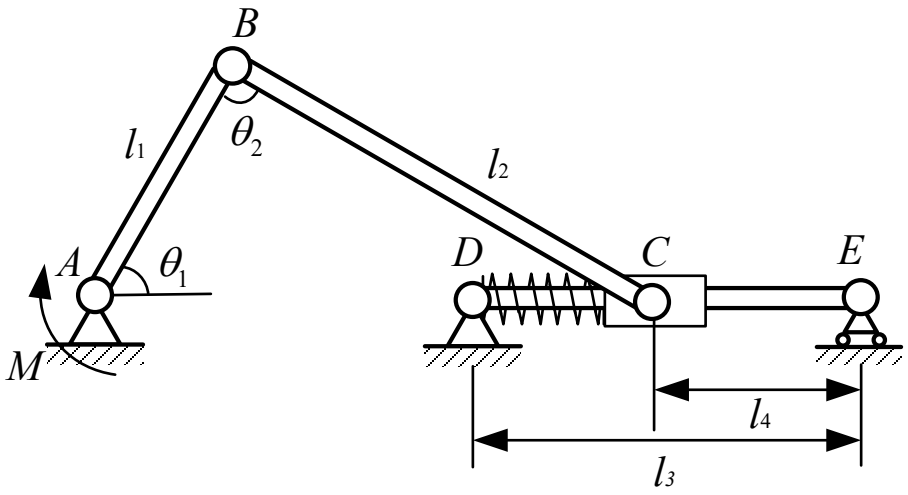

Fig. 5 A crank-slider system